AJNR

Gadolinium-DTPA-Enhanced MR Imaging of the Postoperative Lumbar Spine: Time Course and Mechanism of Enhancement

Jeffrey S. Ross, Richard Delamarter, Mark G. Hueftle, Thomas J. Masaryk, Masamichi Aikawa, John Carter, Carolyn VanDyke and Michael T. Modic

AJNR Am J Neuroradiol 1989, 10 (1) 37-46
http://www.ajnr.org/content/10/1/37

Gadolinium-DTPA–Enhanced MR Imaging of the Postoperative Lumbar Spine: Time Course and Mechanism of Enhancement

Jeffrey S. Ross[1]
Richard Delamarter[2]
Mark G. Hueftle[1]
Thomas J. Masaryk[1]
Masamichi Aikawa[3]
John Carter[2,3]
Carolyn VanDyke[1]
Michael T. Modic[1]

To define the time course and mechanism of enhancement of epidural fibrosis after gadolinium-DTPA (Gd-DTPA) injection, we undertook a three-part study in humans and dogs with epidural scar after spine surgery. First, the dynamic in vivo contrast-enhancing properties of epidural scar were assessed by using sequential fast (18-sec) spin-echo sequences after contrast injection. Epidural scar in dogs rapidly enhanced; peak enhancement (101%) was 6 min after injection, with a slower decline toward baseline to 45% after 44 min. Epidural fibrosis in patients followed a similar pattern, with a maximum enhancement of 73% after 5 min. Paraspinal muscle had a lower peak enhancement in both patients (36%) and dogs (22%). Second, vascular injection in two dogs with India ink demonstrated multiple small vessels throughout the epidural scar. Third, light and electron microscopy was performed on epidural scar obtained at reoperation in both patients and dogs. Light microscopy showed multiple small capillaries scattered throughout a background of collagen. Electron microscopy demonstrated a wide variation in the junctions between endothelial cells ranging from "tight" to "loose." Regions of endothelial discontinuity were also visualized.

This study suggests that Gd-DTPA diffuses rapidly into the extravascular space in epidural scar, with a slower, net movement toward the intravascular compartment as the agent is renally filtered. The contrast agent transgresses the endothelium through "leaky" intercellular junctions and areas of endothelial discontinuity.

Scar is commonly misconceived as a mass of inert collagen representing the terminus of the healing process. In reality, scar is a dynamic, metabolically active material. This activity and vascularity have been used to some advantage with the administration of iodinated contrast material to enhance scar but not disk [1, 2]. This method is technically demanding, and has not achieved widespread use. We have previously shown that MR imaging is an effective technique in making the distinction between epidural fibrosis (scar) and recurrent disk herniation when gadolinium-DTPA (Gd-DTPA) is used in a way analogous to the use of iodinated contrast material [3]. Immediately after IV injection of Gd-DTPA, epidural scar is seen to enhance, while disk material does not enhance. However, the optimum timing for MR imaging after Gd-DTPA injection in the postoperative patient and the reason for such intense scar enhancement have not been elucidated. In an effort to define the time course and mechanism of the enhancement in epidural fibrosis, we undertook a three-part study in humans and animals with epidural scar after spine surgery: (1) vascular injection with India ink in dogs was performed to define the microvascular anatomy of the epidural scar, (2) light and electron microscopy of human and dog epidural fibrosis was performed to assess the scar vascularity and endothelial ultrastructure, and (3) the dynamic in vivo contrast-enhancing properties of Gd-DTPA and epidural scar were assessed by using sequential fast (18-sec) spin-echo sequences after injection of contrast material.

This article appears in the January/February 1989 issue of *AJNR* and the April 1989 issue of *AJR*.

Received March 25, 1988; accepted after revision July 12, 1988.

[1] Department of Radiology, University Hospitals of Cleveland, Case Western Reserve School of Medicine, 2074 Abington Rd., Cleveland, OH 44106. Address reprint requests to J. S. Ross.

[2] Department of Orthopaedic Surgery, University Hospitals of Cleveland, Case Western Reserve School of Medicine, Cleveland, OH 44106.

[3] Department of Pathology, University Hospitals of Cleveland, Case Western Reserve School of Medicine, Cleveland, OH 44106.

***AJNR* 10:37–46, January/February 1989**
0195–6108/89/1001–0037

Materials, Subjects, and Methods

Animal Model

Six adult female beagle dogs (12–14 kg) underwent laminectomy at the L6–L7 level with Silastic banding of the dural tube at the level of the cauda equina 5 months before the Gd-DTPA studies. The banding was performed as part of an unrelated study on cord compression. Four dogs were imaged with MR, and tissue samples were subsequently removed at reoperation for the purpose of light and electron microscopy. Two dogs were used for the India ink vascular preparations. All animals were eventually sacrificed with an overdose of pentobarbital. Epidural scar has previously been shown to consistently form after laminectomy in dogs [4].

Patient Population

Thirty patients were enrolled in an open-label pilot study that used Gd-DTPA in patients with failed back surgery syndrome; the clinical results of that study are described elsewhere [3]. Dynamic MR studies were performed in three patients from this group, the methods of which are described more fully under Imaging Schemes and Pulse Sequences. In 13 patients in this group, signal-intensity measurements of intervertebral disks were obtained before and after contrast enhancement (see the Disk Enhancement section under Data Analysis). Recurrent disk herniation and surrounding scar, which were diagnosed in four patients, were confirmed at surgery.

Imaging Schemes and Pulse Sequences

Imaging experiments were performed on either a 1.0- or 1.5-T superconducting magnet.*

Four dogs were anesthetized with IV sodium pentobarbital, intubated, and placed supine within a 21-cm-diameter resonator coil centered over the lower lumbar spine. Immediately after acquisition of a precontrast axial image through the region of laminectomy, the dimeglumine salt of Gd-DTPA† was injected as a bolus (0.1 mmol/kg) into a forefoot vein without changing the position of the dog within the coil. The IV tubing was rapidly flushed with normal saline.

The dynamic MR studies were obtained by using a standard spin-echo sequence, 70/17 (TR/TE). This allowed a single slice (thickness, 10 mm) with two excitations to be performed every 18 sec. With the addition of software recycling time, images could be obtained approximately every 30 sec. Images were obtained every 30 sec for the first 5 min after injection of contrast material, then every 10 min up to 45 min total. There were 128 phase-encoded cycles. During image acquisition, TR, TE, and field of view were held constant.

Similar dynamic studies were performed in three patients with the failed back surgery syndrome in the first 5 min after administration of contrast material (0.1 mmol/kg Gd-DTPA‡). Precontrast MR images demonstrated abnormal epidural tissue suggestive of scar in all three cases. A single axial level for the dynamic MR study was chosen on the basis of these images. The administration protocol permitted a maximum contrast injection rate of 10 ml/min. Additional fast spin-echo sequences were then interleaved between the clinical images (approximately one image every 7–10 min). Images obtained for clinical diagnosis of scar or recurrent disk herniation were also used for signal-intensity measurements and consisted of pre- and postcontrast T1-weighted sagittal and axial images, 400/15, with a slice thickness of 4 mm and a 256 × 256 matrix.

* Magnetom, Siemens Medical Systems, Iselin, NJ.
† Schering AG, Berlin, W. Germany.
‡ Berlex Laboratories, Cedar Knolls, NJ.

Data Analysis

Scar.—Signal-intensity values were measured on the precontrast and each postcontrast image in regions of interest (ROIs) over epidural scar and the paraspinal musculature by using a cursor and graphic display device in both dogs and humans. The ROIs covered 0.1 cm^2 and were held constant in position and size while the pre- and postcontrast signal intensities of each area were measured. Pixel counts ranged from 30 to 50, but were held constant for any one set of images. Percent contrast enhancement was calculated by using the following formula:

$$\text{enhancement} = \frac{\text{postcontrast SI} - \text{precontrast SI}}{\text{precontrast SI}} \times 100.$$

where SI = signal intensity.

Standards were not included on the dog studies because of the difficulty in maintaining correct position and signal intensity with the field dropoff adherent with the use of surface coils. Corn oil standards were placed along the edge of the surface coil in three human patients studied, and these standards showed no signal variation between images.

Disk enhancement.—In 13 patients, similar signal-intensity measurements were obtained on the pre- and postcontrast studies in ROIs over the L3–L4, L4–L5, and L5–S1 intervertebral disks. These measurements were obtained from the central portions of the parent intervertebral disk on sagittal T1-weighted images. Pixel size and methodology were as described above for scar analysis. The postcontrast sagittal images were obtained approximately 5–15 min after injection of contrast material. Percent enhancement was calculated and compared for operated and nonoperated disk levels.

In four patients surgically proved recurrent disk herniations were surrounded by epidural fibrosis. In these cases, signal-intensity measurements and percent enhancement were obtained over the enhancing epidural scar and the central herniated disk material on precontrast axial T1-weighted images as well as on early (1–10 min) and late (33–58 min) postcontrast images.

Signal intensities of scar and paraspinal muscle after administration of contrast material were tested, as appropriate, for significant difference by means of Student's t test. A score of $p < .05$ was considered significant.

Vascular Studies

Two dogs were sacrificed and exsanguinated. Subsequently, the abdominal aorta was infused with a 1:1:1 mixture of latex, India ink, and water. The whole lumbar spine was then harvested, fixed in formalin (48 hr), dehydrated in 100% ethanol, and cleared in methyl salicylate. The epidural soft tissues were carefully dissected from the dura at the site of laminectomy for subsequent photography.

Specimen Acquisition

For the human studies, one of us was present during the operation and guided the surgeon to collect specimens as defined by the MR studies. Tissue specimens were obtained at reoperation in both humans and dogs. In general, wide laminectomies were performed, allowing good visualization of the epidural structures and precise tissue localization. A similar approach was used for collection of tissue specimens in dogs.

All areas of epidural fibrosis (in patients and laboratory animals) prepared for microscopy demonstrated enhancement on MR after IV injection of Gd-DTPA. In all patients, initial surgery had been performed at least 6 months before. Areas of epidural fibrosis anterior or lateral to the dural tube were removed from seven patients during reoperation. These were immediately placed into the appropriate fixative. Portions of posterior and lateral epidural fibrosis were surgically removed from four dogs and immediately fixed for light and electron microscopy.

Fixations

Light microscopy.—Samples were fixed in 10% formaldehyde and embedded conventionally in paraffin. These samples were stained with hematoxylin and eosin.

Electron microscopy.—Samples were fixed in 2.5% glutaraldehyde buffered to pH 7.4 in 0.1 M sodium cacodylate and 7.5% sucrose for a minimum of 24 hr. Postfixation was performed with 1% osmium tetroxide for 1 hr. Specimens were then dehydrated in graded ethanols and embedded in Epon 812. One-micron-thick sections were examined by light microscopy, which were stained with methylene blue. Portions of interest were then cut with the use of diamond knives and stained with uranyl acetate. Observations were made with a JEM 100 CX electron microscope.

Results

The resolution of the dynamic spin-echo sequences permitted delineation of the vertebral bodies, thecal sac, epidural scar, paraspinal musculature, and other bony structures such as sacroiliac joints. In dogs, before administration of contrast material, the epidural scar was uniformly seen as a homogeneous area of intermediate signal intensity abutting the thecal sac and extending posteriorly a variable distance into the paraspinal musculature. After administration of Gd-DTPA, the epidural scar enhanced rapidly, with a peak enhancement (101%) on images acquired 6 min after injection and a slower decline toward baseline to 45% enhancement after 44 min (Figs. 1 and 2). Paraspinal musculature followed a similar pattern, although the peak enhancement at 4 min was only 22%. The postcontrast scar intensity values were significantly different from their respective postcontrast muscle values ($p < .005$).

In patients, the appearance of scar before contrast administration was of intermediate signal adjacent to the thecal sac (Fig. 3). After injection of Gd-DTPA, the scar enhanced in a pattern similar to that seen in dogs, with a maximum enhancement of 73% after 5 min. The enhancement decreased to

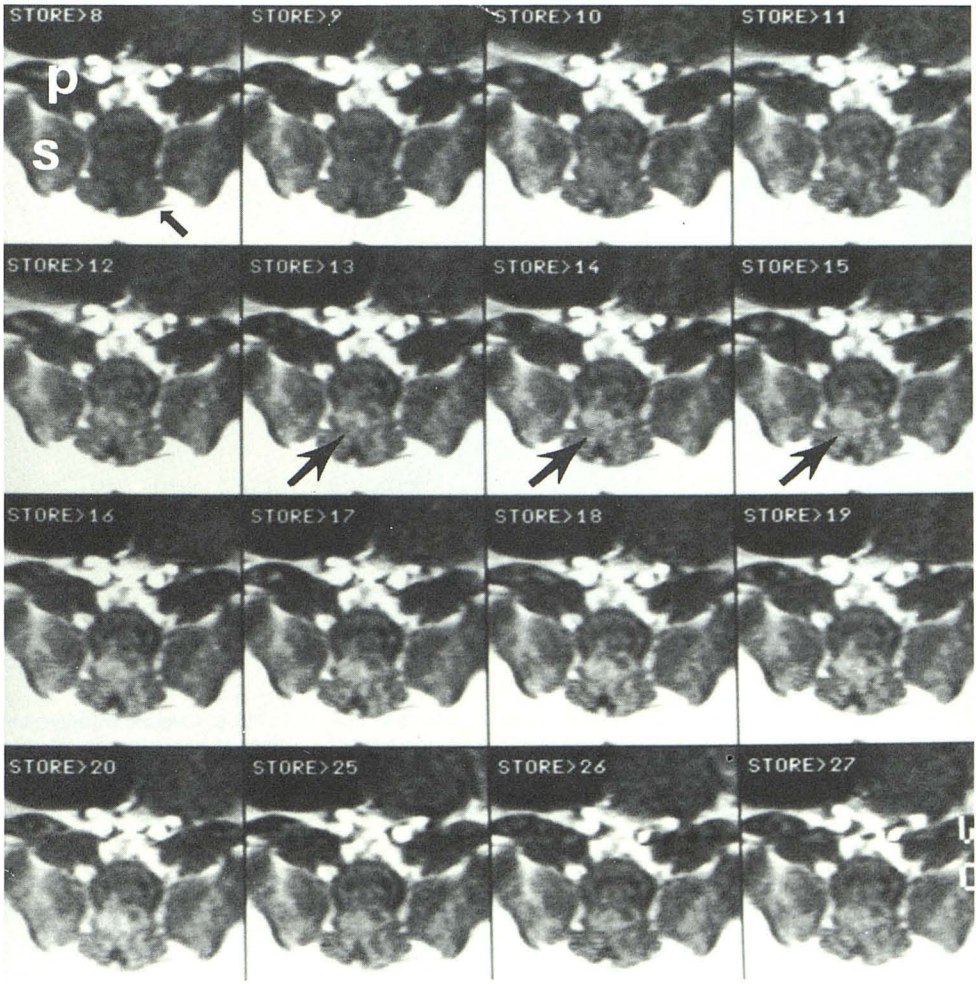

Fig. 1.—Enhancement of dog epidural scar.

***Image 8* (top left), Precontrast image shows epidural soft tissue (*arrow*) to be of low signal, with indistinct thecal sac. Pelvic bones (S) and psoas muscles (P) are well seen.**

***Images 9–20* were obtained every 0.5 min after administration of Gd-DTPA. Note rapid and marked enhancement of epidural scar (*arrows*). Thecal sac becomes more well defined.**

***Images 25–27* (lower right), obtained 25, 26, and 27 min after injection, show decreased intensity within epidural scar.**

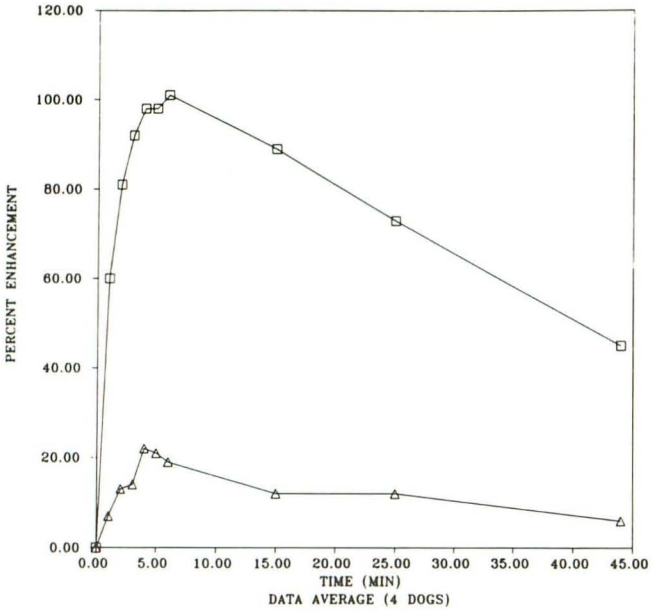

Fig. 2.—Gd-DTPA enhancement in dog epidural scar and muscle. There is rapid enhancement of scar (*top curve*) over the first 6 min, with a slower decrease over the next 38 min. Muscle enhancement (*lower curve*) is much less, although peak time is similar.

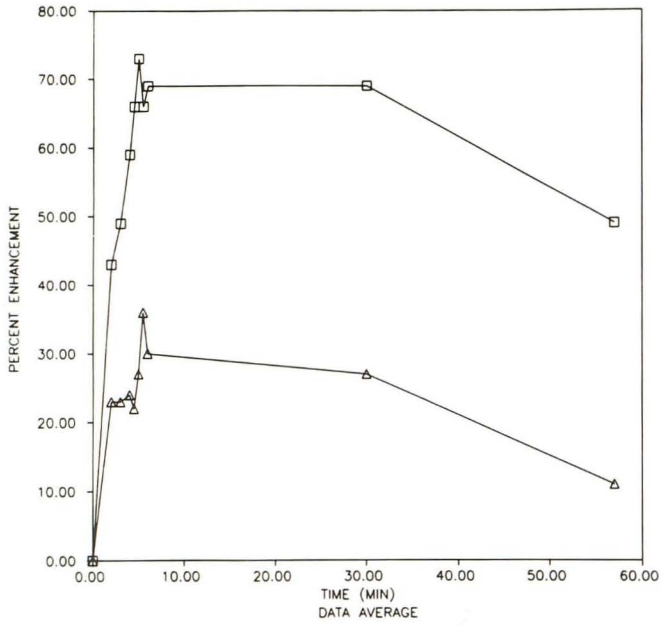

Fig. 3.—Enhancement of epidural scar. Sagittal T1-weighted images.
***A*, Precontrast image shows large soft-tissue signal mass contiguous with L5–S1 disk space.**
***B*, Postcontrast image shows enhancement of scar surrounding large disk herniation (*arrows*). (Surgically proved.)**

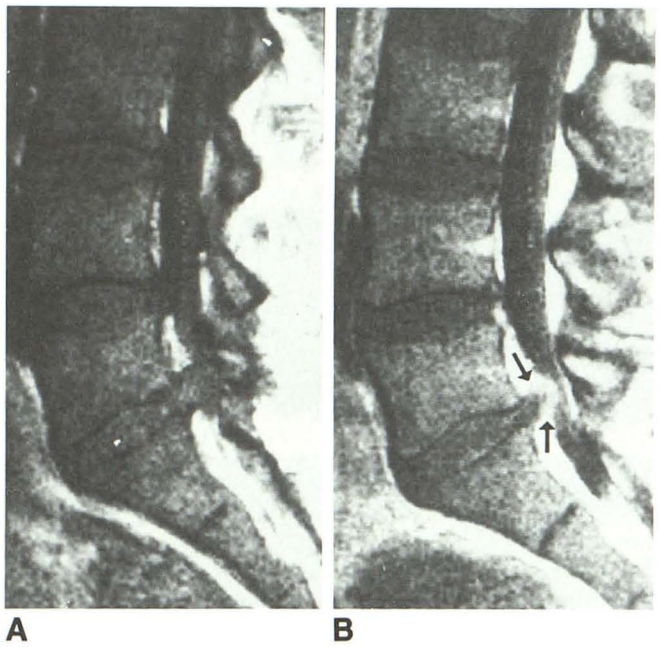

Fig. 4.—Gd-DTPA enhancement in human scar and muscle. Scar enhancement (*top curve*) follows a course similar to that in dogs, with a peak around 6 min and subsequent slower decline. Muscle follows a similar pattern, but with less overall intensity. Curves are averages from signal-intensity values of three patients with enhancing epidural scar.

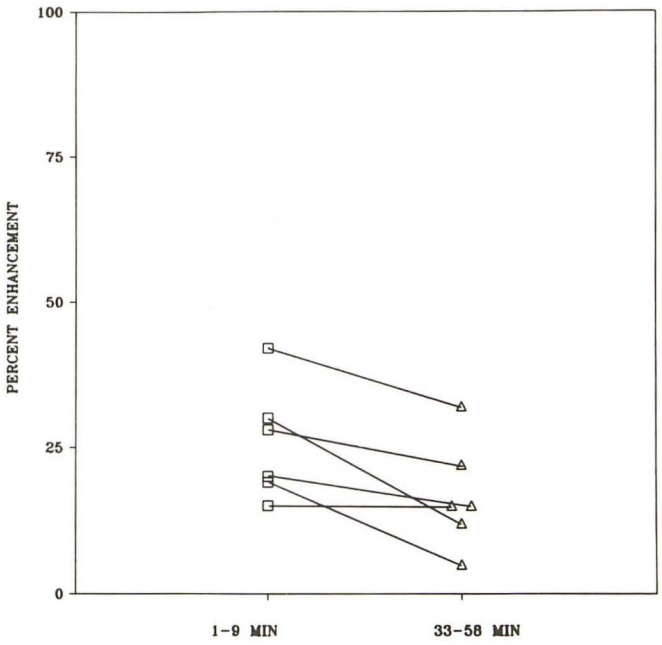

Fig. 5.—Muscle enhancement in six patients derived from signal intensities on spin-echo clinical images. Mild degree of enhancement is seen initially, with slow decrease by 33–58 min, similar to fast spin-echo data.

49% after 57 min. Paraspinal musculature had a lower peak enhancement (36%) after 5.5 min with a decrease to 11% after 57 min (Fig. 4). The postcontrast scar intensity values were significantly different from their respective postcontrast muscle values ($p < .005$). As a check on the fast spin-echo enhancement of paraspinal muscle, in six patients signal intensities were obtained from ROIs over paraspinal muscle on the pre- and postcontrast clinical axial T1-weighted im-

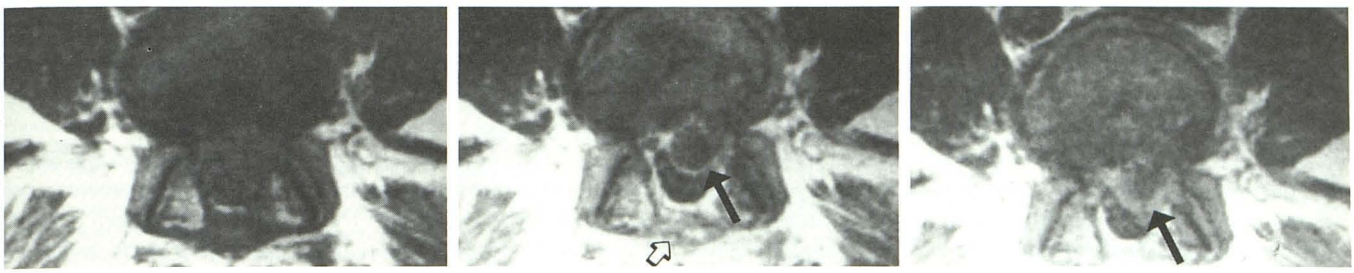

Fig. 6.—Late enhancement of disk herniation.
***A*, Preoperative axial T1-weighted MR image shows indistinct thecal sac and posterior laminectomy scar.**
***B*, Immediate postcontrast image shows enhancement of scar tissue surrounding large nonenhancing disk herniation (*solid arrow*). Posterior scar also enhances prominently (*open arrow*).**
***C*, Late postcontrast image shows smudging of scar/disk herniation interface with enhancement involving disk periphery (*arrow*). (Surgically proved.)**

ages. These enhancement values followed those seen with the fast spin-echo sequences (Fig. 5).

In four patients post–Gd-DTPA images showed enhancement surrounding a recurrent disk herniation. Subsequently, these were all proved histopathologically to be disks "wrapped" in scar after reoperation (Fig. 6). In these patients, the percent enhancement was calculated from ROIs over the enhancing scar, as well as over disk on the postcontrast early and late axial T1-weighted clinical images. The disk material either remained the same intensity or, in three of four cases, increased in signal on the late study. Peridiskal scar signal intensity was more variable, being increased, decreased, or unchanged with time (Fig. 7).

In certain cases, the central aspect of the intervertebral disk (not disk herniation) enhanced. In 13 patients the percent enhancement was obtained from the pre- and postsagittal clinical images for the L3, L4, and L5 disks. Three intervertebral disks at previously operated levels showed marked enhancement (Fig. 8).

Vascular Injection

The vascular preparations in two dogs showed multiple small vessels extending throughout the epidural scar (Fig. 9).

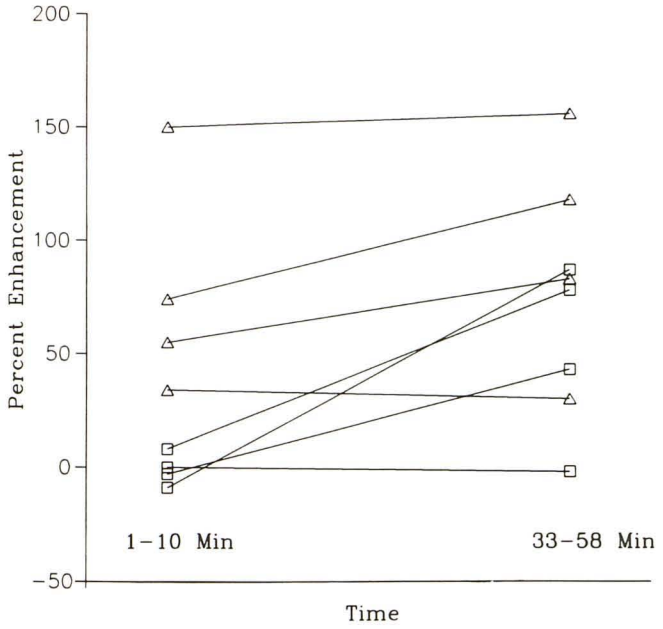

Fig. 7.—Enhancement of disk herniations. Early and late postcontrast enhancement percentages of peridiskal scar (*triangles*) and disk herniations (*squares*) in four patients. Enhancement is seen to occur in three disk herniations by the late study.

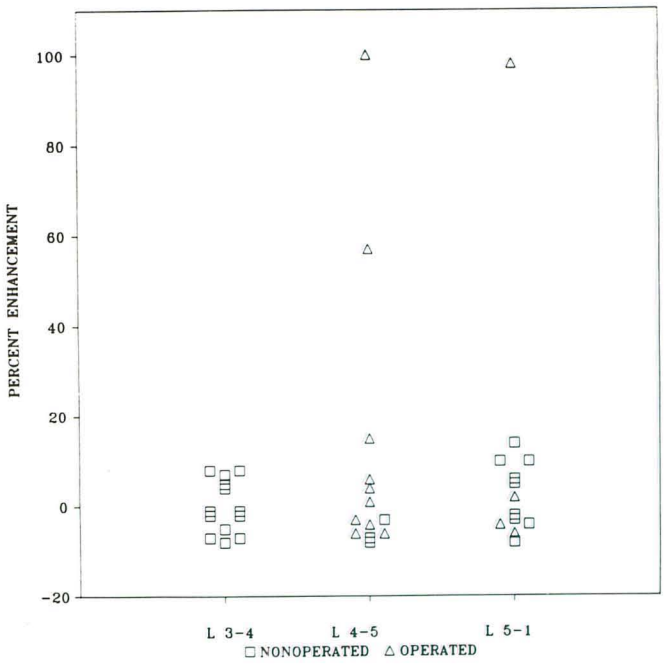

Fig. 8.—Enhancement of central intervertebral disk for operated and nonoperated levels. Levels that enhance markedly had been operated previously (n = 13). Signal intensities were obtained 5–15 minutes after injection.

Light Microscopy

Light microscopy of epidural scar from four dogs and seven humans showed scattered fibrocytes, capillaries, and abundant collagen (Fig. 10). In two patients, the scar had two components. One component consisted of plump fibroblasts with multiple small vessels similar to granulation tissue. This tissue surrounded one disk herniation (Fig. 11). The second component showed scanty vessels and fibrocytes, with abundant collagen forming parallel wavy rows representing mature scar.

Electron Microscopy

Electron microscopy was performed in specimens of scar from two humans and three dogs. These showed three principal findings:

1. True tight junctions (zonulae occludens), where the outer leaflets of the adjoining endothelial cell membranes converged to form a single fused line. These varied in size from a small band of membrane fusion (Fig. 12A) to a focal point of membrane apposition (Fig. 12B). These variations were present in both human and dog scar tissue.

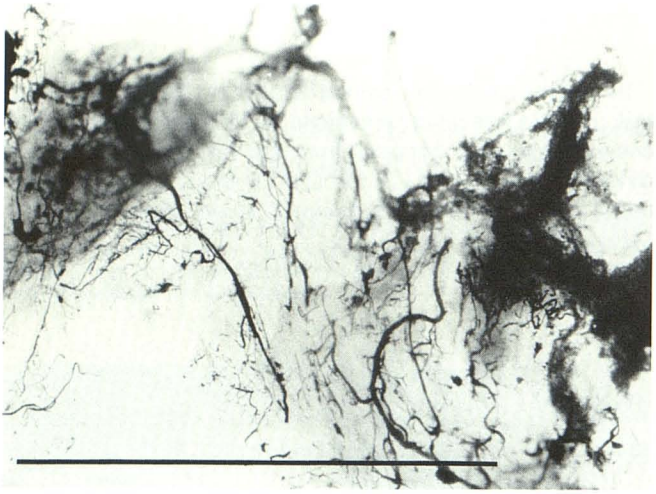

Fig. 9.—Epidural dog scar, India ink vascular injection. Multiple small vessels are distributed throughout scar. Bar represents 1 cm.

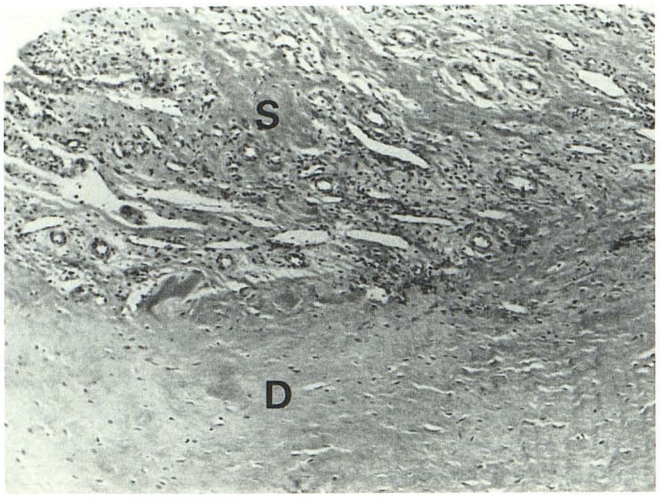

Fig. 11.—Peridiskal scar (same patient as in Fig. 6). Light micrograph shows vascular granulation tissue (S) surrounding avascular disk material (D) (anulus fibrosus). (H and E)

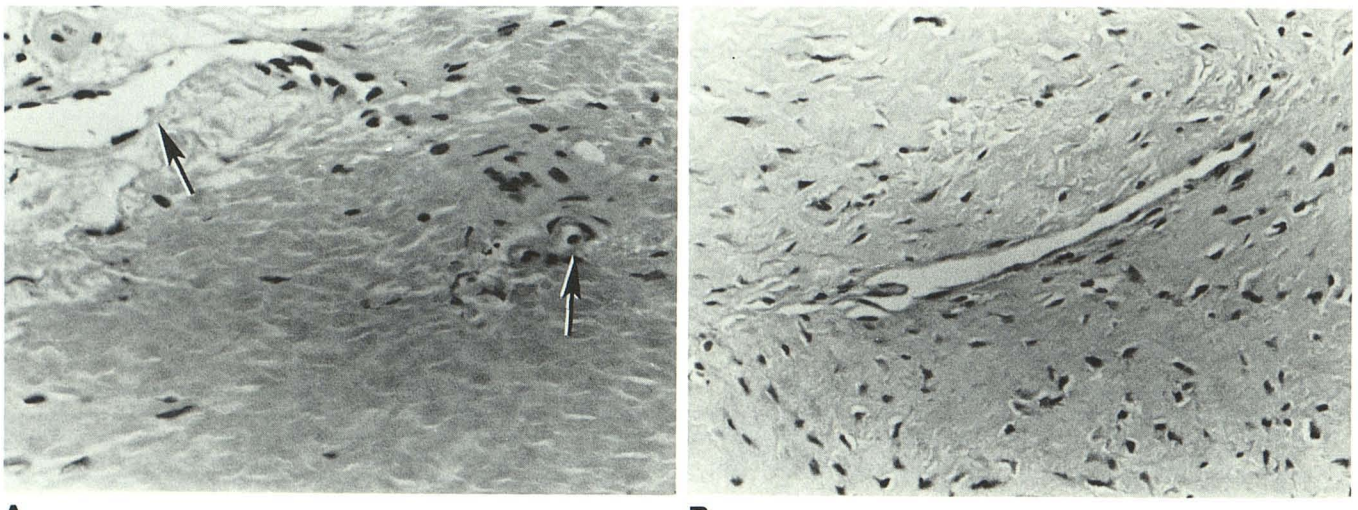

Fig. 10.—Light micrographs of epidural scar. (H and E)
***A*, Human scar. Abundant collagen and several capillaries (*arrows*). (Same patient as in Fig. 3.)**
***B*, Dog scar. Collagen and occasional capillaries, similar in appearance to human scar tissue.**

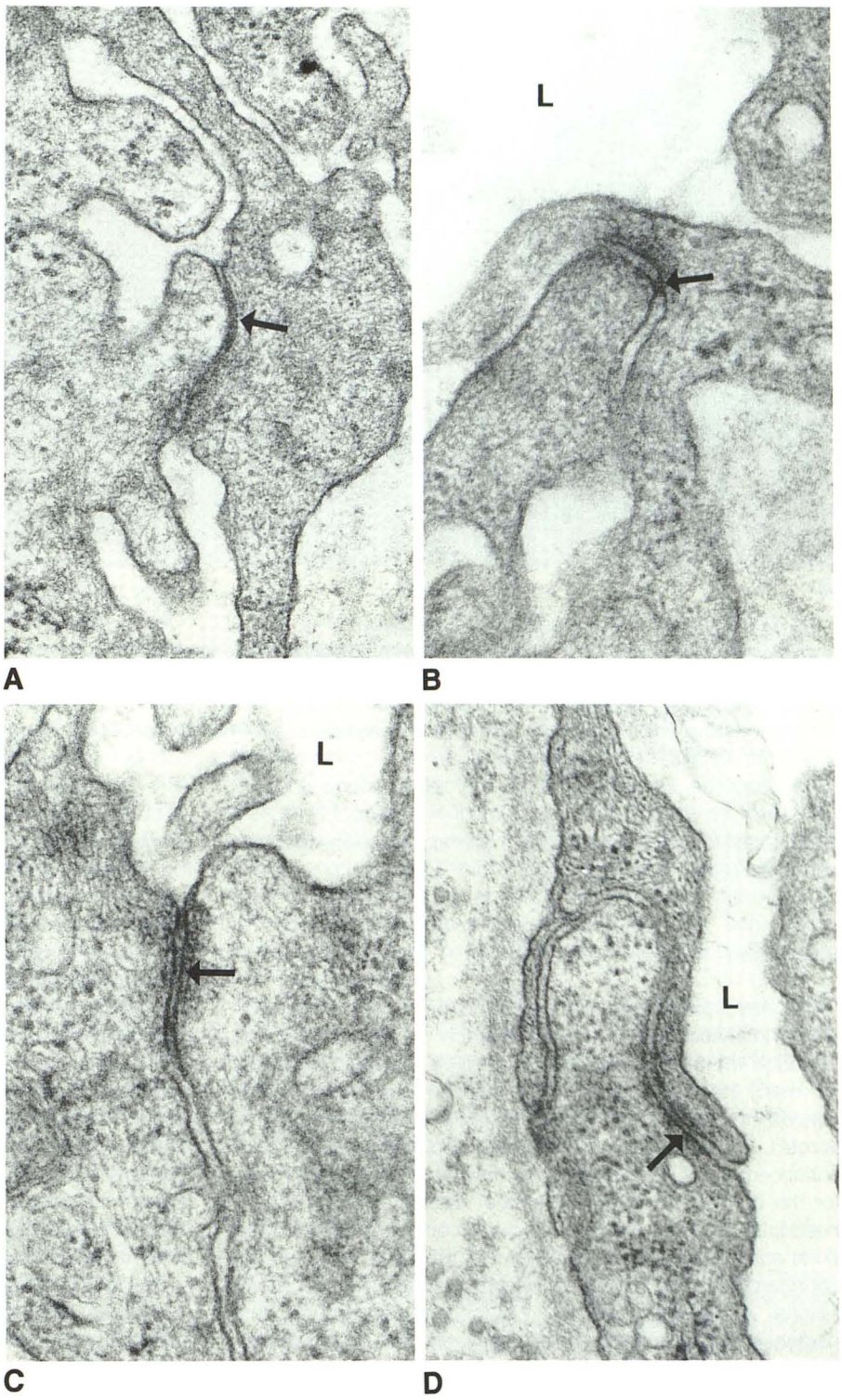

Fig. 12.—Electron micrographs of human (*A–C* [same patient as in Figs. 3 and 10A]) and dog (*D*) scar endothelial junctions.

***A*, Tight junction (*arrow*) shows linear, electron-dense area representing fusion of inner membranes of adjacent endothelial cells. (×99,000)**

***B*, "Focal" tight junction (*arrow*) shows small area of membrane contact. L = lumen. (×99,000)**

***C*, "Open" junction (*arrow*) shows slight increased electron density along cell membranes at luminal surface (L), but no areas of membrane contact. (×99,000)**

***D*, Dog "open" junction (*arrow*). Appearance of adjacent cell membranes is similar to that in *C*. (×70,000)**

2. "Loose" tight junctions, where the outer leaflets approached each other but did not fuse (Figs. 12C and 12D). The loose junctions were also visualized in human and dog samples.

3. Intercellular gaps, where there was a wide space between the endothelial cell membranes extending from lumina to basement membrane (Fig. 13). The endothelial cells themselves were otherwise normal in appearance, as were the

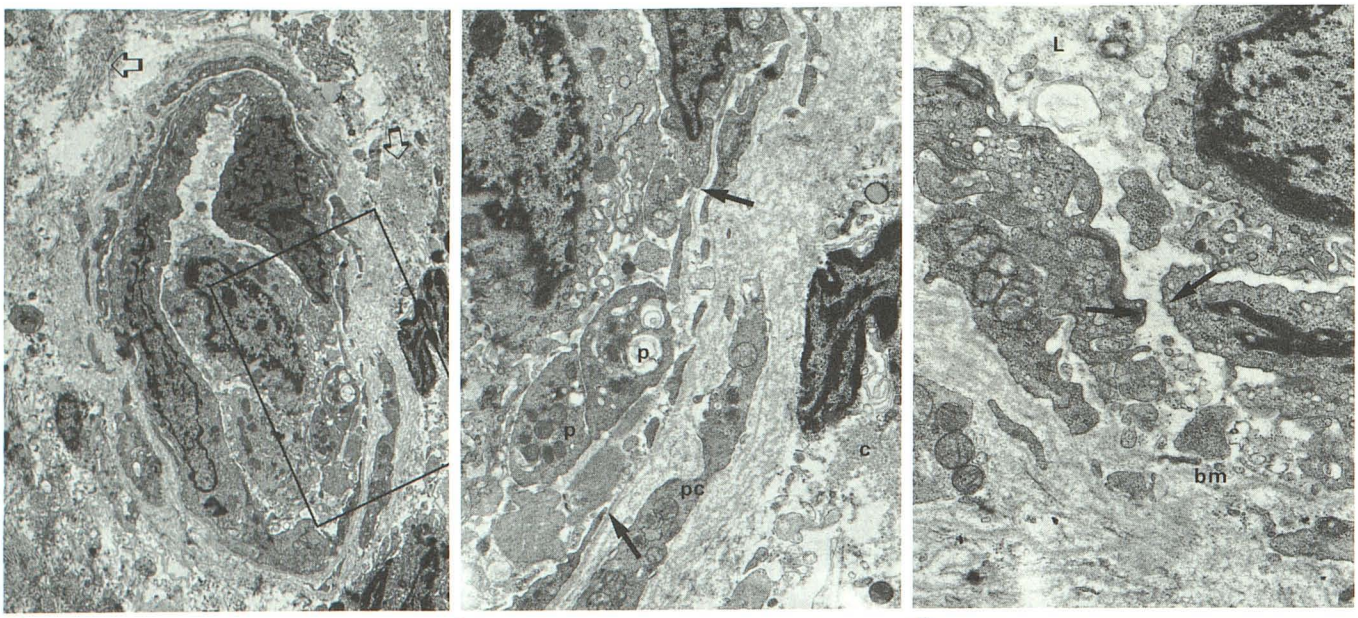

Fig. 13.—Dog epidural scar: discontinuous endothelium.
***A*, Electron micrograph of scar capillary. *Box* denotes region of higher magnification in *B*. Note abundant collagen in extracellular space (*arrows*). (×6600)**
***B*, Higher magnification shows ends of adjacent endothelial cells (*arrows*), with only basement membrane in intervening space. P = platelets; pc = pericytes; c = collagen. (×16,500)**
***C*, Different area of endothelial discontinuity. Ends of adjacent endothelial cells (*arrows*) are separted by small space, connecting the lumen (L) directly to basement membrane (bm). (×25,000)**

pericytes and the interstitium. Abundant collagen was present surrounding the vessels.

Discussion

We have previously described the effectiveness of Gd-DTPA in evaluation of the failed back surgery syndrome. Although the biodistribution of Gd-DTPA has been explored for many normal and abnormal tissues, no reports exist concerning the time course of enhancement within epidural fibrosis. In general, three things are necessary for contrast enhancement of any tissue: (1) a vascular supply, (2) a route for the contrast material out of the vasculature, and (3) an interstitial space for sequestering the contrast material. Epidural scar has all of these attributes. Epidural scar has an abundant vascular supply, as shown by the India ink preparations. A potential pathway out of the vasculature was demonstrated by electron microscopy, and the large interstitial or extracellular space was apparent from the light and electron microscopy.

Electron microscopic studies have shown that there are at least four potential passive pathways for molecules through normal endothelium [5]. The smallest is the 0.3- to 0.4-nm hydrophilic pore in the cell membrane. Although this pathway is crucial to ion and water movement between and into the endothelial cells, it is less important in transendothelial transport than are the larger pathways, because of its hydraulic resistance. The next largest pathways are the intercellular channels, or tight junctions, where under normal conditions the largest molecules that can pass are 2–4 nm. Large molecules such as albumin (4.2 nm and mol wt, 59,000) or horseradish peroxidase (mol wt, 40,000) may be transported through either pinocytotic vesicles or even larger channels. These larger channels would include fenestrated or discontinuous endothelium, as exist in the renal glomeruli or bone marrow, respectively [6].

Our electron microscopic findings suggest that there are two major routes for egress of the small molecule of Gd-DTPA. One is through tight junctions or variants thereof. The zonula occludens closes or seals adjacent cells, which reduces diffusion [7, 8]. These types of junctions allow the creation of gradients between the lumen and the underlying tissues. However, the sealing capacity of tight junctions is quite variable, and relates to cell function. Tissues that need to maintain a steep ionic or osmotic gradient have junctions so tight as to block the movement of small electrolytes and water. "Leakiness" has been related to the freeze-etch morphology of the tissues; "very tight" junctions exhibit a deep zonula occludens with many areas of membrane fusion, while leaky junctions consist of at most one area of fusion [9]. Our electron microscopic observations suggest that the capillaries in scar consist of "leaky" tight junctions with either single areas of fusion or no direct membrane contact. Further, these junctions are relatively short in the apical-basal direction. The second major route for escape of contrast material is the large intercellular gaps. These focal areas of endothelial discontinuity would provide relatively direct access of contrast

material from the lumen into the interstitial space. Discontinuous capillaries normally are found only in organs adapted for free passage of large molecules into and out of the blood; that is, liver, spleen, and bone marrow. In regenerating tissue, endothelial cells within new blood vessels in retina and iris have been shown to be "leaky" to fluorescein and low-molecular-weight tracers secondary to fenestrated capillaries and open intercellular junctions [6]. The leaky junctions and intercellular gaps observed in the endothelium of epidural fibrosis would seem to provide a basic structure-function correlation with Gd-DTPA enhancement.

The biodistribution and kinetics of DTPA–metal ion complexes have been reported for normal tissues [10–14]. The chelates are distributed throughout the extracellular space and are rapidly eliminated by glomerular filtration. Gd-DTPA does not appear to cross intact cell membranes. Gd-DTPA dimeglumine is a small molecule (mol wt, 938) and is similar in size to diatrizoate (mol wt, 600) and iothalamate. This study and others [14–17] suggest that Gd-DTPA diffuses rapidly into the extravascular space. After the equilibration of Gd-DTPA between the intra- and extravascular compartment, the net movement is toward the intravascular compartment, since the agent is renally filtered. Our enhancement curves with Gd-DTPA for scar are very similar to those of the extravascular compartment curves previously described for iothalamate [18]. The increase in the signal intensity of scar tissue would support the theory that tissues with relatively large extravascular spaces and long T1 relaxation times will enhance conspicuously [15, 19, 20]. Certainly, scar tissue, with its abundant collagen, fits this category. Although the overall pattern of enhancement is similar for muscle and epidural scar, there was a qualitative increase in enhancement of scar over muscle with time. This could potentially reflect (1) more vascularity within scar tissue or (2) larger extracellular spaces within scar tissue. Muscle, being an extremely metabolically active tissue, has a large vascular supply and is unlikely to be the cause of the low differential enhancement, as contrasted to epidural scar. However, muscle does have a relatively small extracellular space when compared with scar. The small extracellular space in muscle would not allow the sequestration of contrast material to the same extent as would the large collagen-filled extravascular space in epidural fibrosis.

Our pathologic findings in disk herniations surrounded by scar that enhanced on the late MR studies showed little or no vascularity within the herniations. Although the mechanism of enhancement of disk herniation and intervertebral disk remains speculative, three possibilities should be considered: (1) diffusion of contrast material from the vascular peridiskal scar into the herniation with time, (2) enhancement within intervertebral disks could be secondary to diffusion via vascularized scar from previous curettage of the disk space during surgery, or (3) granulation tissue associated with severe degenerative change. In this group of patients, only the intervertebral disks that were previously curretted showed enhancement. Of course, previous surgical curettage does not mean the parent disk must invariably enhance.

Certain areas of this study deserve further comment. It is highly unlikely that the electron microscopic features of epidural scar could be ascribed to fixation artifact. Great care was taken to immediately immerse small tissue samples in the fixative. The structure of the other intracellular organelles (such as nuclei, mitochondria, and endoplasmic reticulum) was well defined on the same images and were without obvious fixation artifact. Further, regions of intimate cell-to-cell contact involved in ion exchange (gap junctions) were visualized in our specimens, suggesting adequate fixation of all junctional complexes. The potential for sampling error in the histopathologic studies remains a problem, especially with the electron micrographs. Although the variations in endothelial junctions were seen in both human and dog epidural scar, the discontinuous endothelium was seen by electron microscopy only in dog scar. Whether this variation in endothelial structure actually exists in human scar remains unknown. The enhancement curves of Gd-DTPA might be hampered by the inability to bolus the contrast agent in humans. To what degree, if any, this affected the curves is unknown, but it was also unavoidable due to the drug protocol. We have not directly defined the route of egress of Gd-DTPA into epidural fibrosis. Only autoradiographic electron microscopic techniques would show the course of diffusion of the contrast agent.

One puzzling aspect of this study is the fact that there was rapid egress of contrast material into both scar and paraspinal muscle, while scar has been shown to have "open" junctions and discontinuous endothelium. This fact may be related to the gross assessment of vascular permeability that dynamic MR represents. Small differences in capillary permeability probably are not detected with this technique, as opposed to a more sensitive and invasive technique such as measurement of hydraulic conductivitiy [21]. However, our hypothesis concerning the permeability of scar endothelium parallels the findings of Giacomelli et al. [22], who found that the permeability of subendocardial capillaries to horseradish peroxidase could be accounted for by larger-sized interendothelial clefts (i.e., open junctions).

In conclusion, we have defined open junctions and areas of discontinuous endothelium within epidural scar. Given the known size of the molecule, its time course of enhancement, and the potential routes for diffusion, we conclude that Gd-DTPA reaches the capacious extracellular space in scar via the "leaky" junctional complexes.

REFERENCES

1. Braun IF, Hoffman JC, Davis PC, Landman JA, Tindall GT. Contrast enhancement in CT differentiation between recurrent disk herniation and postoperative scar. *AJNR* **1985**;6:607–612, *AJR* **1985**;145:785–790
2. Teplick JG, Haskin ME. Intravenous contrast enhanced CT of the postoperative lumbar spine: improved identification of recurrent disk herniation, scar, arachnoiditis, and diskitis. *AJNR* **1984**;5:373–383, *AJR* **1984**;143:845–855
3. Hueftle M, Modic MT, Ross JS, et al. Lumbar spine: postoperative MR imaging with Gd-DTPA. *Radiology* **1988**;167:817–824
4. LaRocca H. The laminectomy membrane: studies in its evolution, characteristics, effects and prophylaxis in dogs. *J Bone Joint Surg [Br]* **1974**;56-B(3):545–550
5. Weinbaum S. Mathematical models for transport across the endothelial cell layers. *Ann NY Acad Sci* **1983**;416:92–114
6. Tripathi RC, Tripathi BJ. Functional ultrastructure of endothelium. *Bibl Anat* **1977**;16:307–312

7. Farquhar MG, Palade GE. Junctional complexes in various epithelia. *J Cell Biol* **1963**;17:375–412
8. Frizzel RA, Schultz SG. Ionic conductances of extracellular shunt pathways in rabbit ileum. *J Gen Physiol* **1972**;59:318
9. Claude P, Goodenough DA. Fracture faces of zonulae occludentes from "tight" and "leaky" epithelia. *J Cell Biol* **1973**;58:390–400
10. Stevens E, Rosoff B, Werner M, Spencer H. Metabolism of the chelating agent diethylenetriamine pentaacetic acid (C 14-DTPA) in man. *Proc Soc Exp Biol Med* **1962**;111:235–238
11. Hauser W, Atkins HL, Nelson KG, Richards P. Technetium-99m DTPA: a new radiopharmaceutical for brain and kidney scanning. *Radiology* **1970**;94:679–684
12. Hosain F, Reba RC, Wagner HN. Ytterbium-69 diethylenetriaminepentaacetic acid complex. *Radiology* **1968**;91:1199–1203
13. Hagan PL, Chauncey DM, Halpern SE, Ayers PA. Tc-99m thiomalic acid complex: a nonstannous chelate for renal scanning. *J Nucl Med* **1977**;18:353–359
14. Strich G, Hagan PL, Gerber KH, Slutsky RA. Tissue distribution and magnetic resonance spin lattice relaxation. Effects of gadolinium-DTPA. *Radiology* **1985**;154:723–726
15. Brasch RC, Weinmann HJ, Wesley GE. Contrast-enhanced NMR imaging: animal studies using gadolinium-DTPA complex. *AJR* **1984**;142:625–630
16. Boudreau RJ, Burbridge S, Sin S, Lohen MK. Comparison of the biodistribution of manganese-54 DTPA and gadolinium-153 DTPA in dogs. *J Nucl Med* **1987**;28:349–353
17. Wolf GR, Burnett KR, Goldstein EJ, et al. Contrast agent for magnetic resonance imaging. In: Kressel HY, ed. *Magnetic resonance annual.* New York: Raven, **1985**:231–266
18. Newhouse JH. Fluid compartment distribution of intravenous iothalamate in the dog. *Invest Radiol* **1977**;12(4):364–367
19. Wiendorf HP, Felix R, Laniado M, Schorner W, Claussen C, Weinmann HJ. A new contrast agent for magnetic resonance imaging. *Radiat Med* **1985**;3:7–12
20. Hamm B, Wolf KJ, Felix R. Conventional and rapid MR imaging of the liver with GD-DTPA. *Radiology* **1987**;164:313–320
21. Renkin EM. The Microcirculatory Society Eugene M. Landis award lecture. Transport pathways through capillary endothelium. *Microvascular Research* **1978**;15:123–135
22. Giacomelli F, Anversa P, Wrener J. Interendothial gap size of subendocardial vs subepicardial capillaries. *Microvasc Res* **1975**;10:38–42